Expanding the Scope of Peropyrenes and Teropyrenes through a Facile $InCl_3$-catalyzed Multifold Alkyne Benzannulation

Journal:	*Organic Chemistry Frontiers*
Manuscript ID	QO-RES-04-2018-000389.R1
Article Type:	Research Article
Date Submitted by the Author:	09-May-2018
Complete List of Authors:	Yang, Wenlong; University of Nevada Reno Kazemi, Rezvan; University of Nevada, Reno, Chemistry Karunathilake, Nelum; University of Nevada Reno Catalano, Vincent; University of Nevada, Reno, Department of Chemistry Alpuche-Aviles, Mario; University of Nevada, Reno, Chemistry Chalifoux, Wesley; University of Nevada Reno,

Journal Name

ARTICLE

Expanding the Scope of Peropyrenes and Teropyrenes through a Facile $InCl_3$-Catalyzed Multifold Alkyne Benzannulation

Received 00th January 20xx,
Accepted 00th January 20xx

DOI: 10.1039/x0xx00000x

www.rsc.org/

Wenlong Yang, Rezvan R. Kazemi, Nelum Karunathilake, Vincent J. Catalano, Mario A. Alpuche-Aviles, and Wesley A. Chalifoux*

Herein, we report a facile synthesis of bay-region-functionalized peropyrenes and teropyrenes through an $InCl_3$-catalyzed double or quadruple benzannulation reaction of alkynes. This method also allows for the formation of persistently twisted, and thus chiral, peropyrenes. In contrast to using Brønsted acids to facilitate the alkyne benzannulation reaction, these $InCl_3$-catalyzed reactions are capable of cyclizing electron-rich, electron-poor, and even alkyl-substituted alkynes; this drastically improves the scope of products that can be accessed. X-ray crystallographic analysis showed that the substituents in the bay-region play an important role, not only in the crystal packing, but also for their chirality in the solid-state. The excellent solubility and broad scope of both the peropyrenes and teropyrenes obtained by this method, enable us to fully study their interesting optical and electrochemical properties for the first time.

Introduction

A relatively simple and efficient method to produce polycyclic aromatic hydrocarbons (PAHs) containing a wide scope of functional groups is important in electronic and optoelectronic device applications.[1] There are some bottom-up synthetic methods which have been widely used for the controlled synthesis of large π-extended PAHs, such as aryl-aryl oxidation reactions (Scholl reaction),[2] transition metal-catalyzed[3] or light-induced[4] C-C arylation reactions. Moreover, the preparation of carbon-rich materials from precursors containing C-C triple bonds is gaining more attention.[5] This is because there is a large thermodynamic driving force for the formation of new C-C bonds that lead to conjugated materials on account of the high energy of the alkyne moieties in the precursors. Alkyne benzannulation reactions[6] have been shown to proceed using a variety of π-Lewis acids,[6c, 7] Brønsted acids,[8] electrophiles,[9] as well as radical reagents.[10] Transition-metal-catalyzed alkyne benzannulation reactions have been applied to the synthesis of pyrene derivatives.[11] Plenty of π-extended pyrene derivatives have been investigated because pyrene is commercially available and relatively easy to chemically modify.[12] Peropyrene and teropyrene, which can be viewed as 1D π-extended analogues of pyrene, are attractive targets for synthesis owing to their interesting properties. For example, peropyrene[13] and its derivatives[14] have been reported as potential singlet fission materials and it has been proposed that their singlet fission properties could be tuned by altering the crystal packing through chemical substitution. However, there are limited methods for the preparation and functionalization of peropyrene.[13,14] Thus, having an easy way to introduce different substituents onto peropyrenes to not only tune their crystal packing behavior, but other physical properties, would be an important contribution to the field. Teropyrenes absorb and emit light at much longer wavelengths than peropyrene,[15] which make them enticing candidates for optoelectronic devices. Recently, we reported the synthesis of bay-region-functionalized peropyrenes and teropyrenes through triflic acid (TfOH) catalyzed alkyne benzannulation chemistry (Fig. 1a).[15-16] This method was also successfully applied to the preparation of soluble narrow graphene nanoribbons.[17] However, efforts from our lab showed that only electron-rich ethynylaryl moieties, such as *p*-alkyloxyphenylethynyl and ethynylthiophene, were effective cyclization candidates. Neither electron-neutral, electron-deficient ethynylaryls, nor alkyl-substituted alkyne moieties gave cyclization products when using Brønsted acids. Therefore, the creation of a new method to synthesize both peropyrenes and teropyrenes from a broad scope of alkyne-substituted precursors is highly desirable. Compared to the limited scope of Brønsted acids catalyzed alkyne benzannulation (Fig. 1a), in this paper, we disclose an $InCl_3$-catalyzed multifold alkyne benzannulation methodology to construct peropyrenes, teropyrenes, as well as chiral peropyrenes, that is tolerant to a wide scope of alkyne substituents; this includes electron-rich, electron-neutral, and electron-deficient ethynylaryl groups and even ethynyl groups terminated with alkyl substituents (Fig. 1b). The substituent effects were studied by UV-Vis, fluorescence, and cyclic voltammetry.

Department of Chemistry, University of Nevada—Reno, Reno, Nevada 89557, United States

† Electronic Supplementary Information (ESI) available: Experimental procedures, NMR spectra, X-ray crystallographic data, supplementary absorption and fluorescence spectra, and electrochemistry. See DOI: 10.1039/x0xx00000x

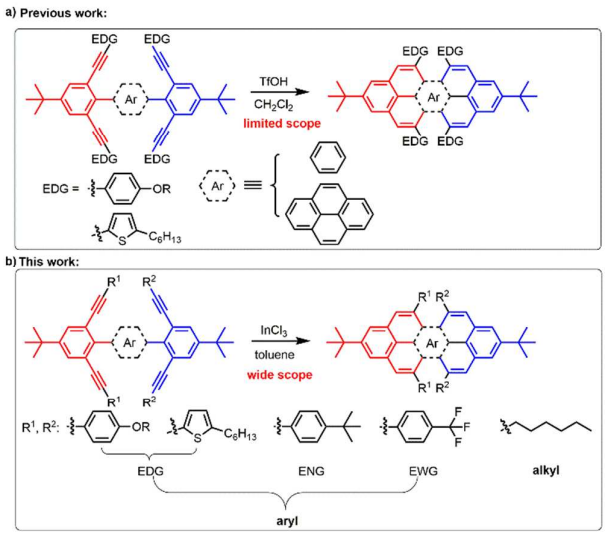

Fig. 1 Synthesis of peropyrenes and teropyrenes through a) triflic acid-catalyzed and b) $InCl_3$-catalyzed benzannulation reactions of alkynes.

Results and discussion

Synthesis

Precursor **1a**, containing electron-rich ethynylaryl substituents, was used as a representative substrate to optimize the benzannulation reaction conditions. Seven different Lewis acid catalysts with the same loadings (30 mol%) were screened in toluene at 100 °C for 12 hours and the results are summarized in Table 1 (entries 1-7). Alkyne benzannulations using Au(I),[11b,18] Au(III),[7d] Pt(II),[7e] Ru(II),[7e] and In(III),[7g] catalysts have been reported to make functionalized PAHs and heteroaromatics. We observed that none of the Au(I) catalysts gave cyclized product **2a** (entries 1-3, Table 1). $AuCl_3$ as a catalyst resulted in trace amounts of mono-cyclized intermediate[15] along with a significant amount of starting material (entry 4). Compared to Au(I) and Au(III) catalysts, In(III) catalysts exhibited higher catalytic ability for this transformation. It was important to point out that after one of the two alkynes reacts to produce the mono-cyclized intermediate, this generates a rigid planar system and makes the second alkyne cyclization more difficult.[15,17] Thus, our reported double cyclization, via a planar intermediate, is different (and more difficult to do) than previously reported $InCl_3$-catalyzed alkyne benzannulations.[7d,7g] Full conversion of starting material **1a** to peropyrene **2a** was observed in the presence of both $In(OTf)_3$ and $InCl_3$, where peropyrene **2a** was isolated in 73% and 88% yields, respectively (entries 5 and 6). We found that $InCl_3$ resulted in a cleaner reaction than $In(OTf)_3$. We also investigated $Sc(OTf)_3$ for alkyne benzannulation, which, to the best of our knowledge, had never been used before for alkyne benzannulations. To our delight, $Sc(OTf)_3$ also worked to give **2a** as the major product along with a trace amount of mono-cyclized intermediate; because this was an inseparable mixture, and since Sc(III) was less effective than In(III), the yield was not determined (entry 7). With $InCl_3$ proving to be an excellent, and cost-effective catalyst for this benzannulation reaction, we decided not to screen any other precious metal catalysts. During our control study (30 mol%, 100 °C, and 12 h reaction time; entry 6), we noticed that the reaction seemed to be complete before 12 h. Upon repeating this reaction, and monitoring it closely, we found that full cyclization was indeed accomplished within 2 hours to provide peropyrene **2a** in 89% yield (entry 8). Decreasing the catalytic loading to 20 mol% required a prolonged reaction time but still gave full conversion of starting material to provide **2a** in good yield (entry 9). With $InCl_3$ being a relatively cheap catalyst, and 30 mol% catalyst loading (15 mol% per alkyne) giving a four-fold increase in reaction rate, we decided to use this catalyst loading for the remainder of the study.

Table 1 Optimization of reaction conditions

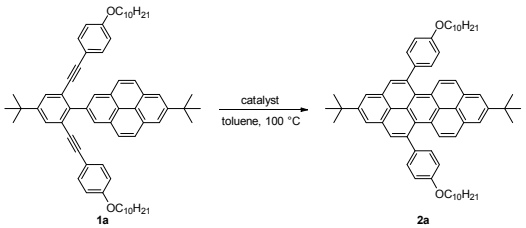

entry	catalyst[a]	time (h)	**2a** (%)[b]
1	$AuCl(PPh_3)$	12	0
2	$AuClP(p\text{-}CF_3\text{-}C_6H_4)_3$	12	0
3	$dppm(AuBr)_2$	12	0
4	$AuCl_3$	12	0
5	$In(OTf)_3$	12	73
6	$InCl_3$	12	88
7	$Sc(OTf)_3$	12	ND[c]
8	$InCl_3$	2	89
9[d]	$InCl_3$	8	83

[a] 30 mol% catalyst loading was used; [b] Isolated yield; [c] Inseparable mixture of **2a** and mono-cyclized intermediate; [d] 20 mol% $InCl_3$ was used. ND = not determined.

With optimized reaction conditions in hand, we began exploring the scope of this reaction. As expected, electron-rich **1b** and **1c** successfully produced peropyrenes **2b** and **2c** in 85% and 86% yields, respectively (entries 1 and 2, Table 2). Interestingly, the yield for **3c** is higher than what was obtained for the benzannulation reaction using TfOH.[16b] It is noteworthy that we were able to successfully synthesize the 4-*tert*-butylphenyl-substituted peropyrene **2d** in 91% yield (entry 3), a reaction that failed with TfOH. However, after treating the electron-deficient precursor **1e** with 30 mol% $InCl_3$ in toluene at 100 °C for 36 hours, we observed the formation of peropyrene **2e** along with a significant amount of mono-cyclized intermediate. Full conversion could not be achieved even after 72 hours at 100 °C using 50 mol% catalyst loading. Finally, by switching to xylene as solvent and running the reaction for 24 hours at 150 °C, we were able to obtain peropyrene **2e** in 72% yield (entry 4). Alkyl-substituted alkyne derivative **1f** was investigated and upon treatment with 30 mol% $InCl_3$ in toluene at 100 °C for 16 hours, alkyl-substituted

peropyrene **2f** was isolated in 87% yield (entry 5). With this new methodology we now have easy access to a broad scope of functionalized peropyrenes – soft materials that are attractive for various electronic and optoelectronic applications.

Table 2 Scope of peropyrenes **2**

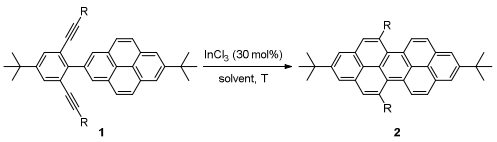

entry	R	solvent	T (°C)	time (h)	yield (%)[a]
1	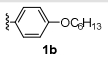 1b	toluene	100	2	**2b**, 85
2	 1c	toluene	100	12	**2c**, 86
3	 1d	toluene	100	12	**2d**, 91
4[b]	 1e	xylene	150	24	**2e**, 72
5	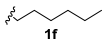 1f	toluene	100	16	**2f**, 87

[a] Isolated yield; [b] 50 mol% catalyst loading.

After the successful preparation of bay-functionalized peropyrenes, we began looking at a four-fold annulation reaction to prepare teropyrene derivatives. After treating precursor **3a** under the optimized reaction conditions for 10 hours, we found that the reaction was incomplete with only some desired product formed. As expected, increasing the catalyst loading to 50 mol% significantly enhanced the reaction rate, with full conversion to product being observed after 8 hours at 100 °C. However, desired teropyrene **4a** was only isolated in 20% yield along with a significant amount of deep purple side product(s) (not characterized)(entry 1, Table 3). Lowering the reaction temperature to 80 °C substantially suppressed the formation of side products with teropyrene **4a** being isolated in a much improved 85% yield (entry 1, Table 3). Under the same reaction conditions, thiophene-functionalized teropyrene **4b** was isolated in 79% yield (entry 3). Interestingly, carrying out the synthesis of teropyrenes **4c** and **4d** at an elevated 100 °C resulted in 90% and 75% yields, respectively, with no apparent side product formation (entries 3 and 4). Unfortunately, we failed to fully cyclize **3e** – containing four *p*-trifluoromethylphenyl substituents – to afford the teropyrene product **4e**. Although partial cyclization was observed, the formation of **4e** was not observed in any appreciable amount, even after prolonged reaction time in xylene at 150 °C with 50 mol% catalyst loading (entry 5). This is likely because, as the alkynes begin to cyclize in succession, the polyaromatic backbone becomes more and more electron-deficient (i.e. less nucleophilic), making the ensuing cyclizations more challenging. Since we were successful in cyclizing two electron-deficient alkynes to make peropyrene **2e** (Table 2), we suspected that we might be able to make a teropyrene that contains at least two electron-poor aryl substituents. To prove our hypothesis, precursor **3f** – containing two *p*-hexyloxyphenylethynyl and two *p*-trifluoromethylphenylethynyl groups – was synthesized. Indeed, teropyrene **4f** – a "push-pull" system – was isolated in 88% yield (entry 6), which proved that the electron density of the backbone can affect the reaction. Since electron-rich alkynes cyclize faster (see Tables 2 and 3), we suspect that one or both of these electron-rich alkyne groups cyclize first to produce a peropyrene intermediate that is relatively electron-rich, which makes cyclization of the remaining electron-poor alkynes more facile (See Scheme S9).

Table 3 Scope of teropyrenes **4**

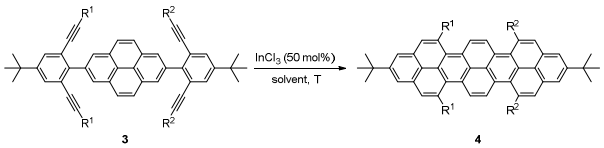

entry	R^1, R^2	solvent	T (°C)	time (h)	yield (%)[a]
1	$R^1 = R^2 =$  3a	toluene	100 80	8 7	**4a**, 20 **4a**, 85
2	$R^1 = R^2 =$  3b	toluene	80	8	**4b**, 79
3	$R^1 = R^2 =$  3c	toluene	100	5	**4c**, 90
4	$R^1 = R^2 =$  3d	toluene	100	10	**4d**, 75
5	$R^1 = R^2 =$  3e	toluene xylene	100 150	24 24	**4e**, 0
6	$R^1 =$ 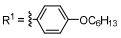 $R^2 =$ 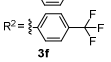 3f	toluene	100	14	**4f**, 88

[a] Isolated yield.

Recently, we reported the first synthesis of chiral peropyrenes through a Brønsted acid-catalyzed four-fold benzannulation reaction of alkynes. This reaction allowed the formation of two new doubly-substituted (thus, helical) bay-regions within the same reaction.[16a] As shown above, teropyrenes could be effectively obtained through an $InCl_3$ catalyzed four-fold benzannulation reaction of alkynes. Therefore, we treated precursor **5a** with 50 mol% of $InCl_3$, and although we observed formation of **6a**, partly cyclized intermediates[16a] could still be observed, even after stirring for 48 hours at 100 °C. Increasing to 120 °C with a 100 mol% of $InCl_3$ (25 mol% catalyst loading per alkyne) provided chiral peropyrene **6a** in 63% yield (entry 1, Table 4). The attempted preparation of chiral peropyrene **6b** – having four thiophene

groups in the bay-positions – failed, with significant decomposition being observed with prolonged reaction time (entry 2). Chiral peropyrene **6c**, with four bulky *p-tert*-butylphenyl groups within the two bay-regions, was obtained in 52% yield (entry 3). Similar to teropyrene **4e**, we failed to fully cyclize the electron-deficient tetrayne precursor **5d** to the corresponding chiral peropyrene **6d**, even at elevated temperature (entry 4). An alkyl-substituted alkyne derivative was also investigated and chiral peropyrene **6e** was successfully isolated, albeit in a modest 8% yield, with the rest being intractable material (entry 5). Very bulky groups were employed to see if we could further twist the peropyrene backbone. We were able to successfully obtain the extremely sterically congested chiral peropyrene **6f** in 59% yield with its structure unambiguously confirmed by X-ray crystallography (vide infra). From the NMR analysis of **6f**, we observed that the rotation of aryl substituents in the bay-positions was significantly restricted, with the *tert*-butyl groups also showing up as broad signals in the ^{1}H NMR spectrum, even at elevated temperature (see Supporting Information). Therefore, it's worthy to point out that this $InCl_3$-catalyzed alkyne benzannulation methodology broadens the scope of products, increases the yields, and also results in cleaner reactions (relative to using Brønsted acids), making it much easier to purify all of these interesting and highly desirable compounds.

Table 4 Scope of chiral peropyrenes **6**

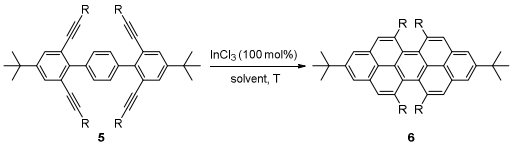

5 **6**

entry	R	solvent	T (°C)	time (h)	yield (%)[a]
1	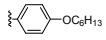 **5a**	toluene	120	24	**6a**, 63
2	 **5b**	toluene	120	24	**6b**, 0
3	 **5c**	toluene	120	36	**6c**, 52
4	 **5d**	toluene xylene	120 150	24 24	**6d**, 0
5	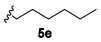 **5e**	toluene	120	48	**6e**, 8
6	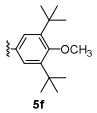 **5f**	toluene	120	24	**6f**, 59

[a] Isolated yield.

Crystal Structures

Single crystals suitable for X-ray crystallographic analysis were obtained for peropyrene **2a**, teropyrenes **4c** and **4d**, and chiral peropyrene **6f**. Compared to the crystal structures of **2b**[15] and **2c**,[16b] the peropyrene backbone of **2a** is slightly less twisted with a bay-region dihedral angle of 13.5° and end-to-end twist angle of 12° (Fig. 2a). Twisted compound **2a** is chiral in the solid-state and packs in a slip-stacked arrangement with its symmetry-generated enantiomer (Fig. 2b) and a minimum interplanar spacing of 3.3 Å (Fig. 2c). Unlike **4a**[15] and **4d**, teropyrene **4c** is chiral in the solid-state (Fig. 2d) and crystalizes with 1.5 molecules (with opposite handedness; red and blue structures in Fig. 2e) in the asymmetric unit. The second half of the partial molecule is generated by a two-fold symmetry operation. The bay-region of the more twisted molecule of **4c** (blue, Fig. 2e) within the asymmetric unit has dihedral angles up to 21°, possibly due to the high steric repulsion of the *tert*-butylphenyl groups (Fig. 2d). Furthermore, the two structures of **4c** in the unit cell have different end-to-end twist angles of 35° and 27° (Fig.e 2e), resulting in a layered packing motif (Fig. 2f). The structure of teropyrene **4d** shows C2v symmetry that is similar to the solid-state structure of **4a**,[15] in which the central naphthyl unit of the PAH is twisted 23° out of planarity with respect to the coplanar ends (Fig. 2g). This twisting is a result of steric repulsion between the alkyl groups and the hydrogen atom in the bay-region of **4d**, resulting in dihedral angles of 23° and 25° (Fig. 2g). More interestingly, **4d** adopts a slip-stacking arrangement (Fig. 2h) with a close interplanar spacing of 3.5 Å (Fig. 2i), making this material a promising candidate in organic electronic and optical devices. We were able to obtain single crystals of **6f** that were suitable for X-ray crystallographic analysis and to probe whether the twist angle could be increased by increasing the sterics (Fig. 2j). Compound **6f** is indeed more twisted **6a**[16a] (by about 3° end-to-end) due to the high repulsion between the 3,5-di-*tert*-butylphenyl substituents, with dihedral angles within the bay-regions of up to 32° and the end-to-end twist angle of 30° (Fig. 2j-k). The π-stacking distance between two aryl substituents within the same bay-region is 4 Å, which is about 1 Å farther apart than that observed in **6a**.[16a] Peropyrene **6f** showed a slip-stacking structure (Fig. 2l), while **6a** adopted a face-to-face molecular packing.[16a]

Journal Name

ARTICLE

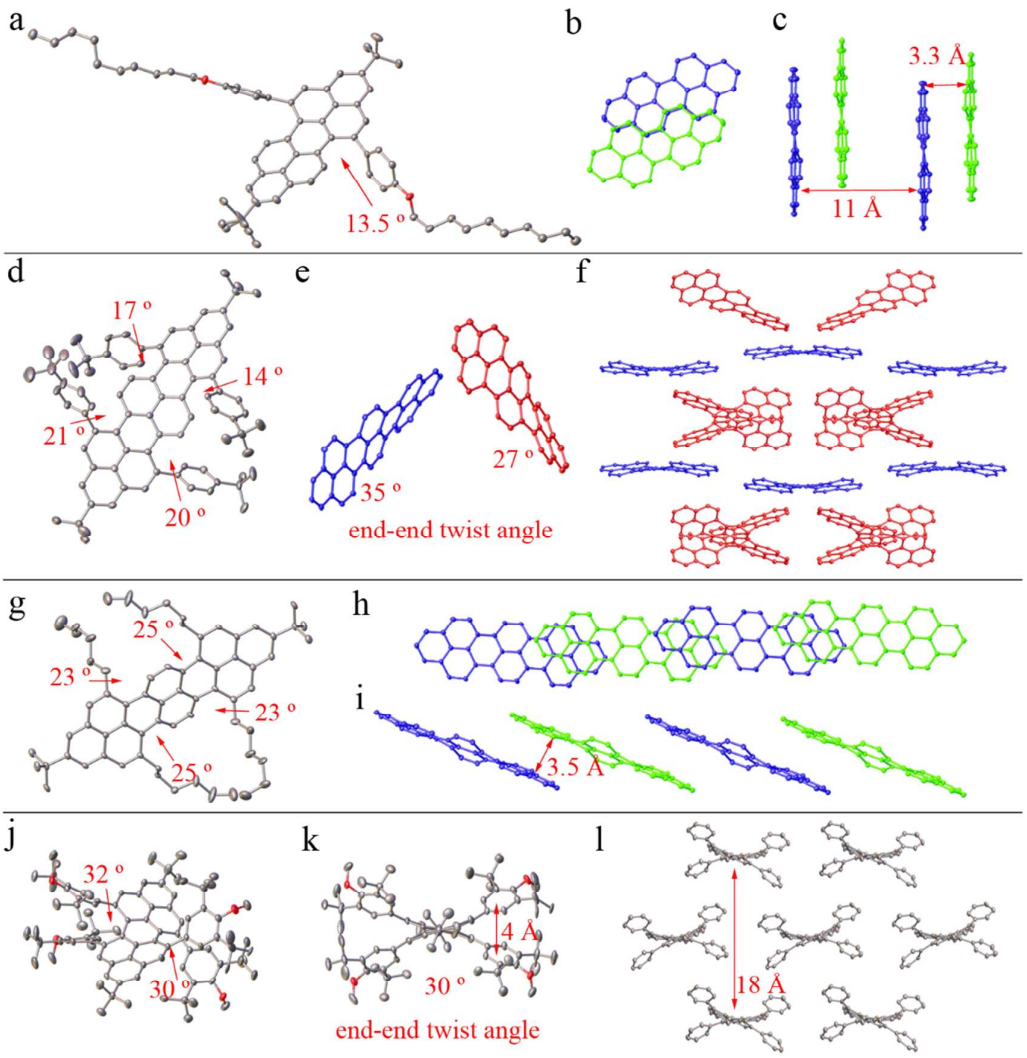

Fig. 2 X-ray structures (ellipsoids at 50% probability, hydrogens removed for clarity) and packing structures (hydrogens and side chains removed for clarity) of (a-c) **2a**, (d) **4c**, which contained 1.5 molecules within the asymmetric cell but only the most twisted molecule is shown, (e-f) the two independent molecules of **4c** with different end-to-end twist angles, (g-i) **4d**, and (j-l) **6f**.

Optical Properties

Our relatively mild method of producing peropyrenes and teropyrenes allows for incorporation of a variety of functionality, leading to these compounds exhibiting excellent solubility in a number of common organic solvents. For the first time, we are now able to study substituent effects on optical and electronic properties of these interesting molecules. The comparison of their UV–vis absorption in toluene solution is shown in Fig. 3. The absorption spectra and the λ_{max} of aryl-substituted peropyrenes **2b-f** are quite similar, which means that electronic communication between the aryl side chains in the bay-region and the peropyrene backbone is negligible (Fig. 3a). This insignificant substituent effect becomes even more evident when comparing the λ_{max} of the aryl-substituted peropyrenes **2b-e** to the alkyl-substituted peropyrene **2f**. The same phenomena were also observed in

the absorption spectra of teropyrenes **4** (Fig. 3b); this being particularly evident when comparing all other teropyrene spectra to the alkyl-substituted derivative **4d** and also to **4f**, which is effectively a push-pull system. These results are in accordance with X-ray analysis, in which the aryl substituents in the bay-region are twisted out of conjugation by 57-68° relative to the PAH backbone, leading to very little orbital overlap. More interestingly, we found that the highly twisted chiral peropyrenes **6** exhibited a ~40 to 50 nm red-shift compared with peropyrenes **2**. This red-shift is also observed for the all alkyl-substituted chiral peropyrene **6e**, albeit to a lesser degree. This suggests that the red-shift is due, at least in part, to twisting of the PAH backbone. In contrast with the results obtained for compounds **2**, we found that the absorption spectra of chiral peropyrenes **6** did shift slightly when varying the substituents on the aryl group (Fig. 3c). This is because the aryl group in the bay-region of **6** have better π-overlap with the PAH backbone, being twisted out of conjugation by 33-37° (less that observed for compounds **2**, vide supra). This increase in conjugation is evident by a red-shift (~20 nm) in UV-vis absorbance in going from the tetraalkyl derivative **6e** to the tetraaryl derivative **6a**. The good solubility of peropyrenes **2** and teropyrenes **4** allows us to study their thin-film absorption properties. Broad absorption bands were observed along with red-shifts in absorbance (10~15 nm) (Fig. S7). The broadening and red-shift observed in the absorbance spectra is a strong indication of intermolecular π-π interactions between these molecules in the solid-state. However, the *tert*-butylphenyl-substituted peropyrene **2d** and teropyrene **4c** had negligible red-shifts in the solid-state (Fig. S7). This can be attributed the bulky substituents causing large packing distances between molecules, leading to weak π-π interactions (as seen in the X-ray packing). The fluorescence spectra were also recorded for all compounds (Fig. S2, S4, and S6). Peropyrenes emit green light and teropyrenes red light, as observed in analogous systems.[15] There were very small Stokes shifts observed for all compounds, which is expected on account of their high rigidity.

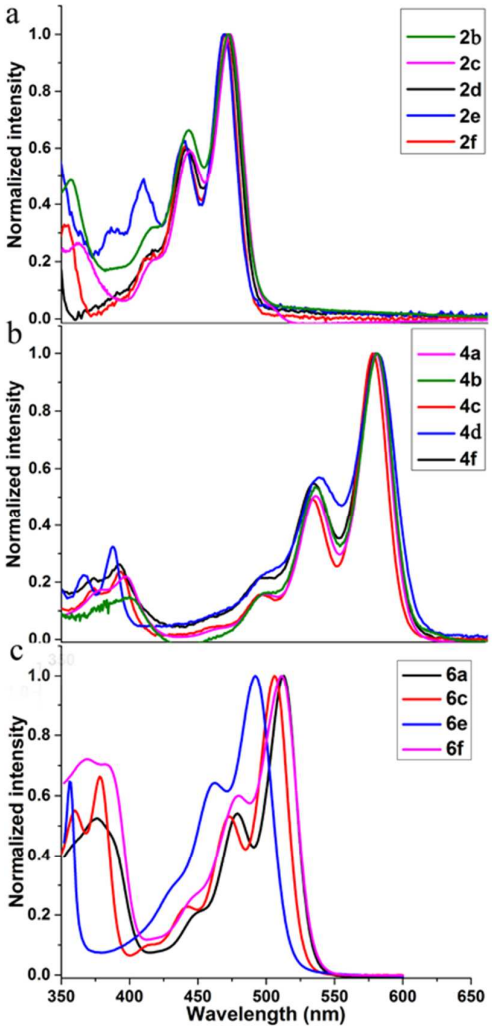

Fig. 3 Normalized UV−vis absorption spectra of a) peropyrenes **2**, b) teropyrenes **4**, and c) chiral peropyrenes **6**, in toluene at room temperature.

Electrochemistry

To the best of our knowledge, the comparison of the electrochemistry of peropyrenes, chiral peropyrenes, and teropyrenes, has not been reported. The electrochemical behavior of peropyrene, chiral peropyrene, and teropyrene compounds were studied using cyclic voltammetry (CV) and the results are summarized in table 5 with CV results of some representative compounds shown in Fig. 4. All the compounds exhibit two reversible peaks for reduction and oxidation reactions, respectively. Herein, we focus on the first reduction and oxidation waves and discuss substituent effects on the bandgap. A complete discussion of the electrochemistry of these compounds will be presented elsewhere. As can be seen in Fig. 4, all compounds show chemically reversible waves for a one-electron reduction and a one-electron oxidation process. The assignment of a one-electron process is justified by the excellent agreement between the digital simulations and the experimental data (Fig. S8 and S9). As expected, the reduction

process became harder for the peropyrene containing electron-rich aryl substituents (**2b**) while it became easier with electron-poor aryl substituents (**2e**) (Fig. 4a). Compared to alkyl-substituted peropyrene **2f**, all aryl-substituted peropyrenes (**2b-e**) exhibited lower HOMO and LUMO energies. However, their bandgaps remain consistent (~2.5 eV). Compared to peropyrene **2b**, chiral peropyrene **6a** showed increased HOMO and decreased LUMO energies (Fig. 4b), which caused a slight decrease of the bandgap (0.1 eV). Similar changes were also observed between **2d** and **6c**. Interestingly, the bandgap of **6e** is also 0.1 eV lower than **2f**. In this case, the alkyl substituents are expected to have a negligible effect on the bandgap; therefore, this result suggests that increasing the twist of the peropyrene core causes the bandgap to decrease. However, we found that the HOMO of the very sterically hindered compound **6f** dramatically decreased while its LUMO remained consistent with other chiral peropyrene derivatives, resulting in a larger bandgap than expected. There is a slight difference (0.21 eV) between the electronic and optical bandgap for **6f**, which suggests there is a slightly higher barrier of electron transfer for this substrate, relative to the other pero- and teropyrene derivatives. We are currently investigating these differences and the effect of twisting in these molecules. Teropyrenes **4** exhibited a smaller bandgap (~2.1 eV) than peropyrenes **2** and **6**, which is clearly shown in Fig. 4c. Compared to **4a**, both reduction and oxidation peaks of **4f** are shifted towards more positive potentials due to the two electron-withdrawing CF_3 groups (Fig. 4c). From this study, we can conclude that altering the substituents in the bay-region can be a method to modulate the HOMO/LUMO levels but has little effect on the bandgap. However, bandgap engineering can be achieved by modulating the conjugation length of the PAH backbone. It is also noteworthy to point out that all of the optical and electrochemical bandgap energies show excellent agreement, except for compound **6f** (as discussed above).

Table 5 Photochemical and electrochemical parameters of compounds **2**, **4**, and **6**.

compound[a]	$E°_{Ox}$/V[b]	$E°_{Red}$/V[b]	E_{HOMO}/eV[c]	E_{LUMO}/eV[c]	$E_{g(EC)}$/eV[d]	λ_{abs}/nm[e]	$E_{g(opt)}$/eV[f]
2b	0.82	-1.68	-5.22	-2.71	2.51	467	2.50
2c	0.86	-1.63	-5.26	-2.77	2.49	469	2.50
2d	0.82	-1.66	-5.22	-2.74	2.52	465	2.53
2e	0.96	-1.56	-5.36	-2.84	2.52	465	2.54
2f	0.77	-1.70	-5.17	-2.70	2.47	468	2.52
4a	0.63	-1.45	-5.03	-2.95	2.08	572	2.07
4b	0.69	-1.37	-5.09	-3.03	2.06	573	2.06
4c	0.64	-1.45	-5.04	-2.95	2.09	569	2.08
4d	0.58	-1.43	-4.98	-2.97	2.01	572	2.05
4f	0.73	-1.38	-5.13	-3.02	2.11	571	2.06
6a	0.76	-1.66	-5.16	-2.74	2.42	506	2.34
6c	0.80	-1.62	-5.20	-2.78	2.42	513	2.34
6e	0.72	-1.66	-5.12	-2.74	2.38	492	2.37
6f	0.87	-1.67	-5.27	-2.73	2.54	511	2.33

[a] The electrochemistry of **2a** was not studied since **2a** and **2b** are similar. [b] Redox potential obtained by digital simulation versus SCE. [c] Calculated according to $E_{HOMO} = -(E_{Ox} + 4.4\ eV)$ and $E_{LUMO} = -(E_{Red} + 4.4\ eV)$. [d] Calculated from redox potentials. [e] Absorption wavelengths of the first absorption onset. [f] Estimated from the UV–vis spectra.

Journal Name

ARTICLE

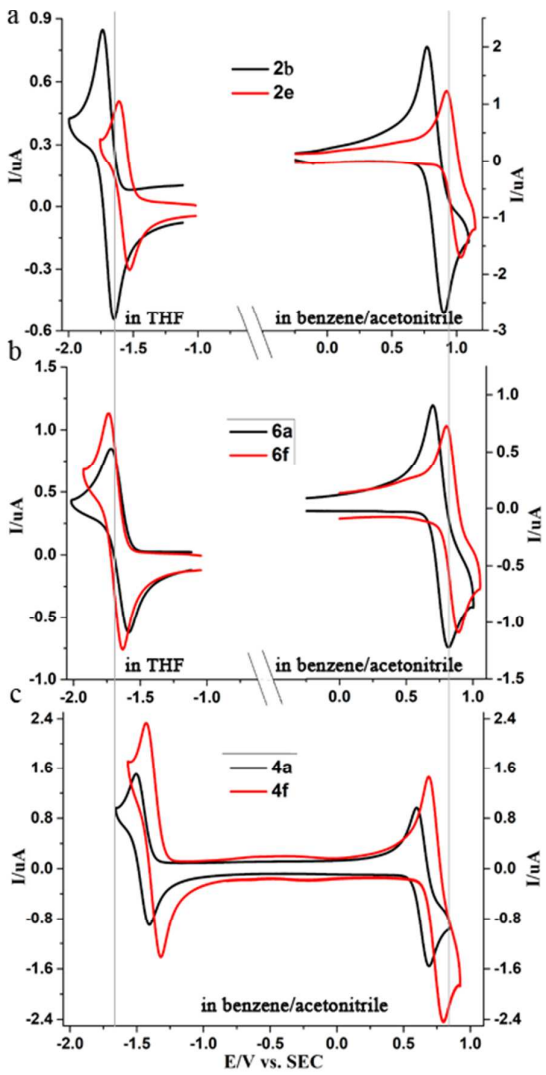

Fig. 4 Cyclic voltammograms of a) **2b** and **2e** in THF (0.4 mM) for reduction and in benzene/acetonitrile (5:1) mixture (0.8 mM) for oxidation, b) **6a** and **6f** in THF (0.4 mM) for reduction and in benzene/acetonitrile (5:1) mixture (0.8 mM) for oxidation, c) **4a** and **4f** in benzene/acetonitrile (5:1) mixture (0.8 mM). 0.1 M TBAP was used as the supporting electrolyte. Gray line (left and right lines are E0 of the first reduction, at 1.686, and oxidation, at 0.824, of **2b**, respectively) added as a guide to the eye to show relative changes in reduction and oxidation energies.

Conclusions

In summary, we have demonstrated that the synthesis of bay-region-functionalized peropyrenes and teropyrenes can be achieved using multifold alkyne benzannulations catalyzed by $InCl_3$. We show that various aryl- and alkyl-substituted alkyne moieties can be cyclized, enabling access to a wide scope of these useful compounds. Incorporation of a broad scope of substituents into these conjugated materials not only allows for tuning of their optical and electronic properties, but also imparts excellent solubility, making these conjugated materials easily processable for a breadth of applications. A decrease in the HOMO–LUMO gap (2.50 to 2.10 eV) from peropyrene to teropyrene was observed from both the optical and electrochemical studies. Within a certain class of PAH (i.e., peropyrene, chiral peropyrene, or teropyrene), small changes in HOMO and LUMO energy levels were observed when varying the bay-region substituents, with the bandgaps remaining essentially constant. There did seem to be an effect on the bandgap energies as a function of the PAH being twisted out of planarity, with bandgaps decreasing as a function of twist angle. X-ray crystallographic analysis showed that the substituents in the bay-regions can effectively tune their crystal packing motifs to modulate the intermolecular π-π interactions. We believe that this new methodology will lead to the development of new functional PAHs, and that these multifaceted studies will attract scientists in other fields to explore their use in electronic and optoelectronic applications.

Conflicts of interest

There are no conflicts to declare.

Acknowledgements

WAC acknowledges the National Science Foundation (NSF) for supporting this work through a CAREER Award (CHE-1555218). MAA thanks the NSF for support through a CAREER Award (CHE-1255387).

Notes and references

1 (a) T. Wöhrle, I. Wurzbach, J. Kirres, A. Kostidou, N. Kapernaum, J. Litterscheidt, J. C. Haenle, P. Staffeld, A. Baro, F. Giesselmann and S. Laschat, *Chem. Rev.*, 2016, **116**, 1139; (b) M. Ball, Y. Zhong, Y. Wu, C. Schenck, F. Ng, M. Steigerwald, S. Xiao and C. Nuckolls, *Acc. Chem. Res.*, 2015, **48**, 267; (c) Y. Shen and C.-F. Chen, *Chem. Rev.*, 2012, **112**, 1463; (d) W. Pisula, X. Feng and K. Müllen, *Adv. Mater.*, 2010, **22**, 3634; (e) J. Wu, W. Pisula and K. Müllen, *Chem. Rev.*, 2007, **107**, 718.

2 (a) K. Y. Cheung, X. Xu and Q. Miao, *J. Am. Chem. Soc.*, 2015, **137**, 3910; (b) T. Fujikawa, Y. Segawa and K. Itami, *J. Am. Chem. Soc.*, 2015, **137**, 7763; (c) J. Liu, B. W. Li, Y. Z. Tan, A. Giannakopoulos, C. Sanchez-Sanchez, D. Beljonne, P. Ruffieux, R. Fasel, X. Feng and K. Müllen, *J. Am. Chem. Soc.*,

2015, **137**, 6097; (d) A. Narita, X.-Y. Wang, X. Feng and K. Müllen, *Chem. Soc. Rev.*, 2015, **44**, 6616; (e) T. Fujikawa, Y. Segawa and K. Itami, *J. Am. Chem. Soc.*, 2016, **138**, 3587; (f) Y. Li, Z. Jia, S. Xiao, H. Liu and Y. Li, *Nat. Commun.*, 2016, **7**, 11637; (g) Y. Sakamoto and T. Suzuki, *J. Am. Chem. Soc.*, 2013, **135**, 14074; (h) K. Kawasumi, Q. Zhang, Y. Segawa, L. T. Scott and K. Itami, *Nat. Chem.*, 2013, **5**, 739; (i) A. Pradhan, P. Dechambenoit, H. Bock and F. Durola, *Angew. Chem. Int. Ed.*, 2011, **50**, 12582; (j) H.-A. Lin, Y. Sato, Y. Segawa, T. Nishihara, N. Sugimoto, L. T. Scott, T. Higashiyama and K. Itami, *Angew. Chem. Int. Ed.*, 2018, **57**, 2874; (k) J. Luo, X. Xu, R. Mao and Q. Miao, *J. Am. Chem. Soc.*, 2012, **134**, 13796.

3 (a) Y. Koga, T. Kaneda, Y. Saito, K. Murakami and K. Itami, *Science*, 2018, **359**, 435; (b) W. Matsuoka, H. Ito and K. Itami, *Angew. Chem. Int. Ed.*, 2017, **56**, 12224.

4 (a) M. Daigle, A. Picard-Lafond, E. Soligo and J.-F. Morin, *Angew. Chem. Int. Ed.*, 2016, **55**, 2042; (b) R. K. Mohamed, S. Mondal, J. V. Guerrera, T. M. Eaton, T. E. Albrecht-Schmitt, M. Shatruk and I. V. Alabugin, *Angew. Chem. Int. Ed.*, 2016, **55**, 12054.

5 (a) E. T. Chernick and R. R. Tykwinski, *J. Phys. Org. Chem.*, 2013, **26**, 742; (b) F. Diederich and M. Kivala, *Adv. Mater.*, 2010, **22**, 803; (c) R. S. Jordan, Y. Wang, R. D. McCurdy, M. T. Yeung, K. L. Marsh, S. I. Khan, R. B. Kaner and Y. Rubin, *Chem*, **1**, 78; (d) I. V. Alabugin and E. Gonzalez-Rodriguez, *Acc. Chem. Res.*, doi:10.1021/acs.accounts.8b00026.

6 (a) W. Yang and W. A. Chalifoux, *Synlett*, 2017, **28**, 625; (b) S. J. Hein, D. Lehnherr, H. Arslan, F. J. Uribe-Romo and W. R. Dichtel, *Acc. Chem. Res.*, 2017, **50**, 2776; (c) H. Arslan, J. D. Saathoff, D. N. Bunck, P. Clancy and W. R. Dichtel, *Angew. Chem. Int. Ed.*, 2012, **51**, 12051.

7 (a) S. Yamaguchi and T. M. Swager, *J. Am. Chem. Soc.*, 2001, **123**, 12087; (b) A. Fürstner and V. Mamane, *J. Org. Chem.*, 2002, **67**, 6264; (c) A. Fürstner and V. Mamane, *Chem. Commun.*, 2003, 2112; (d) V. Mamane, P. Hannen and A. Furstner, *Chem. Eur. J.*, 2004, **10**, 4556; (e) T. A. Chen, T. J. Lee, M. Y. Lin, S. M. Sohel, E. W. Diau, S. F. Lush and R. S. Liu, *Chem. Eur. J.*, 2010, **16**, 1826; (f) J. Carreras, G. Gopakumar, L. Gu, A. Gimeno, P. Linowski, J. Petuškova, W. Thiel and M. Alcarazo, *J. Am. Chem. Soc.*, 2013, **135**, 18815; (g) R. Stężycki, M. Grzybowski, G. Clermont, M. Blanchard-Desce and D. T. Gryko, *Chem. Eur. J.*, 2016, **22**, 5198.

8 M. B. Goldfinger, K. B. Crawford and T. M. Swager, *J. Am. Chem. Soc.*, 1997, **119**, 4578.

9 T. Yao, M. A. Campo and R. C. Larock, *J. Org. Chem.*, 2005, **70**, 3511.

10 K. Pati, C. Michas, D. Allenger, I. Piskun, P. S. Coutros, G. d. P. Gomes and I. V. Alabugin, *J. Org. Chem.*, 2015, **80**, 11706.

11 (a) M. M. Machuy, C. Würtele and P. R. Schreiner, *Synthesis*, 2012, **44**, 1405; (b) T. Matsuda, T. Moriya, T. Goya and M. Murakami, *Chem. Lett.*, 2011, **40**, 40.

12 (a) J. M. Casas-Solvas, J. D. Howgego and A. P. Davis, *Org. Biomol. Chem.*, 2014, **12**, 212; (b) T. M. Figueira-Duarte and K. Müllen, *Chem. Rev.*, 2011, **111**, 7260.

13 V. M. Nichols, M. T. Rodriguez, G. B. Piland, F. Tham, V. N. Nesterov, W. J. Youngblood and C. J. Bardeen, *J. Phys. Chem. C*, 2013, **117**, 16802.

14 (a) K. Uchida, T. Kubo, D. Yamanaka, A. Furube, H. Matsuzaki, R. Nishii, Y. Sakagami, A. Abulikemu and K. Kamada, *Can. J. Chem.*, 2017, **95**, 432; (b) M. Martinez-Abadia, G. Antonicelli, A. Saeki and A. Mateo-Alonso, *Angew. Chem. Int. Ed.*, doi:10.1002/anie.201804453.

15 W. Yang, J. H. S. K. Monteiro, A. de Bettencourt-Dias, V. J. Catalano and W. A. Chalifoux, *Angew. Chem. Int. Ed.*, 2016, **55**, 10427.

16 (a) W. Yang, G. Longhi, S. Abbate, A. Lucotti, M. Tommasini, C. Villani, V. J. Catalano, A. O. Lykhin, S. A. Varganov and W. A. Chalifoux, *J. Am. Chem. Soc.*, 2017, **139**, 13102; (b) W. Yang, J. H. S. K. Monteiro, A. de Bettencourt-Dias and W. A. Chalifoux, *Can. J. Chem.*, 2016, **95**, 341.

17 W. Yang, A. Lucotti, M. Tommasini and W. A. Chalifoux, *J. Am. Chem. Soc.*, 2016, **138**, 9137.

18 A. Davis, D. Walker and J. Howgego, *Synthesis*, 2010, **2010**, 3686.